Near-Infrared-Emitting Hemicyanines and Their Photodynamic Killing of Cancer Cells

Novel Near-Infrared Emitting Hemicyanines and their Photodynamic Killing of Cancer Cells

Mithun Santra, Matthew Owens, Gavin Birch and Mark Bradley*

EaStCHEM School of Chemistry, University of Edinburgh, David Brewster Road, EH9 3FJ, Edinburgh, UK.

ABSTRACT: A series of novel hemicyanine dyes were synthesized starting from the vinyl chloride based cyanine dye IR-780. The new dyes absorbed and emitted in near infrared region, while heavy atom (bromo and iodo) substitution promoted the generation of both singlet oxygen ($^1O_2$) and broader reactive oxygen species (ROS) upon irradiation at wavelengths greater than 610 nm. One hemicyanine dye displayed an outstanding singlet oxygen quantum efficiency (Φ_Δ = 0.8) and was successfully applied in in vitro studies to mimic photodynamic therapy application.

KEYWARDS: hemicyanines, heavy atom, fluorescence, near infrared emitting, photodynamic therapy

INTRODUCTION

Imaging with the aid of fluorescent dyes is a powerful technique for the localization and dynamic monitoring of biomolecules in cells and tissues,[1,2] and has led to the development of many new imaging agents and fluorophores.[3,4] However, fluorophores with short absorption and emission wavelengths can result in significant photodamage/photobleaching during cell and tissue imaging, while short wavelengths also overlap with intrinsic autofluorescence from biomolecules such as flavin, retinol and folic acid.[5,6] Fluorophores that emit in the far red or near-infrared (NIR) wavelength region (650−900 nm) thus have advantages since background autofluorescence is reduced, while the reduced energy minimises photodamage, allowing deeper penetration, albeit 1-2 mm.[7,8] Accordingly the development of new NIR-emitting dyes with desirable optical properties is of great interest.[9,10] There are a number of far-red or NIR (650−900 nm) emitting fluorophores available[11,12] and cyanine dyes are perhaps the best well known, but can have drawbacks such as aggregation in aqueous solution (unless sulfonated),[13] poor photostability, and low quantum yields.[14,15] Hemicyanines (structurally "half of a cyanine dye") absorb and emit in the NIR region, and numerous molecular probes/fluorescent sensing systems have been reported based-on the hemicyanine dyes **HCy-1** or **HCy-2** (Scheme 1).[16,17] However, these hemicyanines have not been explored in great detail with respect to their singlet oxygen generation properties. Herein, we report the design and synthesis of derivatives of hemicyanines including sulfur and heavy atom (bromine, iodine) substitutions with the ambition to allow the generation of cytotoxic reactive oxygen species (ROS) and singlet oxygen ($^1O_2$) upon photo-activation. This was driven by the fact that the incorporation of heteroatoms and heavy atoms into dyes is known to promote the generation of cytotoxic reactive oxygen species (ROS) and singlet oxygen ($^1O_2$) upon photo-activation, a key need in the development of new PDT dyes. The photophysical properties of the new dyes were explored with the best dye, containing a heavy atom, having a singlet oxygen quantum efficiency of 0.8 and demonstrated efficient photocytotoxicity towards cancer cells upon irradiation at 640 nm. To synthesize the new hemicyanine dyes, the procedure reported by Ma was developed.[18,19] Thus, the chloro-substituted cyanine dye (IR-780) were treated with resorcinol, halo-substituted resorcinol or 3-mercaptophenol to give the hydroxyl-substituted hemicyanines (**HCy-OH**) (Scheme 1). The amino-substituted hemicyanines (**HCy-NH$_2$**) were obtained similarly, treating IR-780 with 3-nitrophenol or 3-nitrobenzenethiol followed by reduction with $SnCl_2$ (Scheme 1).

EXPERIMENTAL SECTION

General information of materials and methods. All experiments that were sensitive to moisture or air were performed under a positive pressure of Ar gas in flame-dried glassware equipped with a rubber septum. Solvent and liquid reagents were transferred using Ar-flushed syringes or cannulae. Unless otherwise noted, commercial reagents were purchased from Aldrich, Alfa Aesar, Merck, Acros and other commercial suppliers and were used as received. All reactions were monitored using TLC Merck 60 F_{254} pre-coated silica gel plates. Flash column chromatography was conducted on Merck silica gel 60, 230–400 mesh ASTM. Nuclear magnetic resonance spectra (^{1}H, ^{13}C NMR) were recorded on Bruker AVA500 spectrometer operating at 500 MHz for 1H and 126 MHz for 13C. Chemical shift for 1H NMR spectra is reported as δ in parts per million (ppm) down field from tetramethylsilane (δ 0.0 ppm) using the residual solvent signal as an internal standard: chloroform-*d* (δ 7.26 ppm, singlet), dimethyl sulfoxide-d_6 (δ 2.49 ppm, quintet), methanol-d_4 (δ 3.3 ppm, quintet), water-d_2 (δ 4.67 ppm, singlet). Multiplicities are given as: s (singlet), d (doublet), t (triplet), q (quartet), dd (doublet of doublet), dt (doublet of triplet), m (multiplet). Coupling constants *J* are reported in hertz. The number n of protons for a given resonance absorbance is indicated by nH. Carbon nuclear magnetic resonance spectra (^{13}C NMR) are

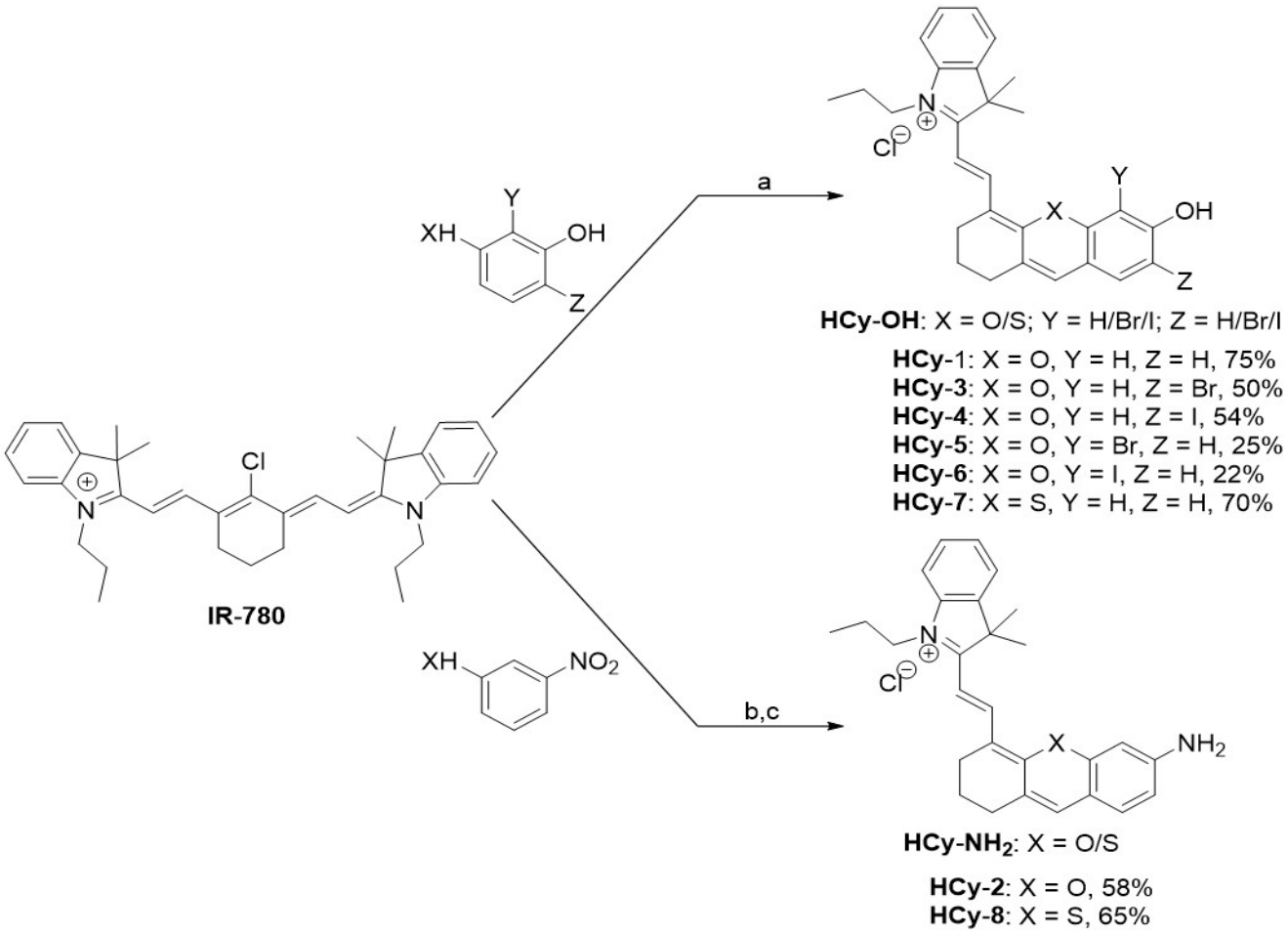

Scheme 1. Synthesis of the hydroxyl-substituted hemicyanine (HCy-OH), and the amino-substituted hemicyanine (HCy-NH_2) with overall synthetic yields. Reagents and conditions: (a) K_2CO_3, CH_3CN, 60–70 °C, 12 h; (b) K_2CO_3, CH_3CN, 4–5 h; (c) $SnCl_2$, conc. HCl, MeOH, reflux, 12 h.

reported as δ in part per million relative to solvent signal: chloroform-*d* (δ 77.7 ppm, triplet), dimethyl sulfoxide-d_6 (δ 39.5 ppm, septet), methanol-d_4 (δ 49.0 ppm, septet). High Resolution Mass Spectra (HRMS) were performed on a Bruker 3.0 T Apex II spectrometer. Each hemicyanine dye was dissolve in EtOH to make 1.0 mM stock solution, and these solution were used for photophysical property studies. UV/Vis absorption spectra were obtained using a HP 8453 spectrophotometer and microplate reader (Synergy HT, BioTek). Fluorescence spectra were recorded on RF-6000 spectro fluorophotometer, SHIMADZU**.**

Determination of Quantum Yields. Fluorescence quantum yields of all hemicyanines (**HCy-1─HCy-8**) were determined using indocyanine green (ICG) in EtOH ($\Phi_F = 0.132$)[20] as a reference fluorophore by comparative method and the quantum yield was calculated according to following equation.

$$\Phi_{(x)} = \Phi_{(ref)} (A_{ref}F_x/A_xF_{ref}) (n_x/n_{ref})^2$$

Here Φ is the fluorescence quantum yield, A is the absorbance of excitation wavelength used, and F is the area under the corrected fluorescence emission curve, n is the refractive index of the solvent used, subscript ref and x refer to reference and to unknown respectively.

Quantification of singlet oxygen generation. To quantify singlet oxygen generation upon light irradiation 1,3-Diphenylisobenzofuran (DPBF) was used as singlet oxygen sensor. All hemicyanines (**HCy-1─HCy-8**, 10 μM) and DPBF (200 μM) were mixed in MeOH. Initially absorption was measured in the dark, and then the mixture was irradiated and absorption was measured at different time intervals. The decrease of absorbance of DPBF with time upon light irradiation indicates the generation of singlet oxygen (colourless 1,2-dibenzoylbenzene). The measurements were performed using a white light source with a 610 nm long-pass glass filter (0.02 W/cm^2). The relative singlet oxygen quantum yields were calculated following literature proceedures.[21,22]

Cytotoxicity study in the dark. HeLa cells were seeded into 96-well plates at a density of 1 x 10^5/well and incubated for 24 h at 37 °C in a humidified atmosphere of 5% CO_2 in air. **HCy-6** in culture medium at various concentrations (1, 5, 10 and 20 μM) was added to the cells and incubated for 24 h before addition of CCK-8 solution to each well of the plate. After a further incubation for 4 h, absorbance at 450 nm was measured using a microplate reader (Synergy HT, BioTek). Cell viability was calculated as a percentage of the absorbance of the untreated control cells. Data were represented as the mean and standard deviation (SD) of three independent experiments.

Cytotoxicity study in presence and absence of light. HeLa cells were thus seeded into 96-well plates at a density of 1 x 10^5 cells/well and incubated for 24 h at 37 °C in a humidified atmosphere of 5% CO_2 in air. Next, the fluorophore solution of

HCy-6 and Methylene blue (**MB**) at various concentrations (0.1, 1.0 and 10 μM) in culture medium were added to the cells. Two sets of plates were prepared. The first set of plates were irradiated by 640 nm LED strips for 5 min (0.01 W/cm^2), and second set of plates were not irradiated by light. The two sets of plates were then incubated for 24 h, followed by the addition of CCK-8 solution to each well. After a further incubation for 4 h, absorbance at 450 nm was measured using a microplate reader (Synergy HT, BioTek). Cell viability was calculated as the percentage of the absorbance of untreated control cells. Data were represented as the mean and standard deviation (SD) of three independent experiments.

Cell culture. HeLa cells were maintained in DMEM supplemented with 10% (v/v) fetal bovine serum (FBS), 100 U/mL penicillin, 100 μg/mL streptomycin, and 2 mM L-glutamine at 37 °C in a humidified atmosphere of 5% CO_2 in air. Cells were passaged when they reached approximately 90% confluence.

Fluorescence microscopic imaging. HeLa cells were seeded on 8-well plates at a density of 3 × 10^5 cells per well in culture media and incubated overnight at 37 °C under 5% CO_2. After overnight culture, HeLa cells were incubated with 5 μM of **HCy-6** or Methylene blue for 2 h, and next irradiated for 5 min with 640 nm LED strips (0.01 W/cm^2). After overnight incubation, the cells were co-stained with LIVE/DEAD TM cell imaging kit (Invitrogen) for 30 min. After washing with PBS, fluorescence images were obtained by Leica DM IL LED Fluo inverted microscopy. Alternatively, HeLa cells were incubated with 5 μM **HCy-6** for 2 h, and next treated with 2′,7′-dichlorodihydrofluorescein diacetate (DCFH-DA, 10 μM) and dihydrorhodamine (DHR, 10 μM) for 30 min. After washing with PBS, cells were irradiated by 640 nm LED strips (0.01 W/cm^2) and their fluorescence images were acquired using Leica DM IL LED Fluo inverted microscopy.

Synthesis of HCy-1. Hemicyanine **HCy-1** was synthesized according to the reported procedure by Ma.[18] To a solution of IR-780 iodide (200 mg, 0.29 mmol, 1.0 equiv.) in CH_3CN (10 mL), resorcinol (82 mg, 0.72 mmol, 2.5 equiv.) and K_2CO_3 (103 mg, 0.72 mmol, 2.5 equiv.) were added in a 50 mL of round-bottom flask. Next the resulting solution was stirred at 55 °C for 6–8 h. Then the reaction was allowed to cool to room temperature, filtered on celite, and washed with CH_2Cl_2. The filtrate was concentrated, and it was subjected to flash chromatography on silica gel (eluent = MeOH/CH_2Cl_2 (1:15)) to afford the desired product as blue solid (101 mg, 75%). HPLC (500 nm) t_R = 4.84 min, purity 98% (ELSD). HR ESI-MS: calculated for $C_{28}H_{30}O_2N$ $[M+H]^+$ m/z 412.22711; found 412.22560.

Synthesis of HCy-2. Hemicyanine **HCy-2** was synthesized according to the reported procedure.[19] The compound was purified by flash chromatography on silica gel (eluent = MeOH/CH_2Cl_2 (1:10)) to afford the desired product as green solid (58%). HPLC (500 nm) t_R = 5.02 min, purity 97 % (ELSD). HR ESI-MS: calculated for $C_{28}H_{31}ON_2$ $[M+H]^+$ m/z 411.24309; found 411.24060. All others hemicyanine dyes were synthesized according to the same procedure as either **HCy-1** or **HCy-2**, and their characterization have been discussed in the supporting information.

RESULTS AND DISCUSSION

Photophysical properties of the hemicyanine dyes. The absorption and emission spectra of all the new hemicyanine dyes were measured in EtOH and showed absorption between 600–800 nm and emission between 700–850 nm with **HCy-7** and **HCy-8** being the two most red-shifted (Figure 1 and Figure S3). Interestingly, all the halo-substituted hemicyanines showed bathochromic shifts compared to **HCy-1**, while the sulfur containing hemicyanines showing a shift of 60–80 nm. Moreover, the absorption spectra for **HCy-6** also showed bathochromic shifts with increasing organic solvent polarity (except DMSO), emitting strongly in EtOH compared to other solvents (Figure S4). The fluorescence quantum yields, optical brightness, and Stokes shifts were determined in EtOH and PBS (pH 7.4) (table 1). The dyes had low to moderate quantum yields (Φ_F <0.07–0.30) depending on both solvent and the substituents, with relatively higher quantum yields in organic solvent compared to PBS e.g. for **HCy-4** Φ_F in EtOH was 0.28, and 0.18 in PBS. The sulfur-substituted hemicyanines had the lowest quantum yield of the series e.g. Φ_F was 0.30 for **HCy-3** whereas Φ_F was 0.09 for **HCy-8** (both in EtOH). These numbers were not surprising as NIR-emitting cyanines and hemicyanines generally have poor quantum yields,[23] while sulfur substitutions are known to decreases the quantum efficiency of many dyes e.g. tetramethylrosamine (TMR) has a quantum yield 0.84, but is 0.21 for TMR–S.[24] All the dyes had very high molar absorptivities (ε = ~10^5), with Stokes shift values between 20–60 nm in EtOH. In comparison with Food and Drug-Administration approved

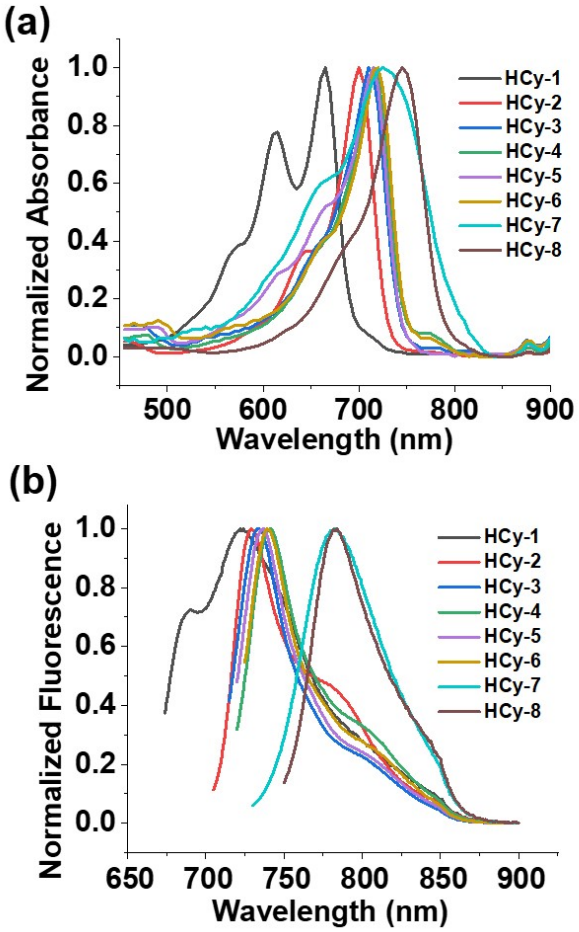

Figure 1. (a) Normalized absorption, and (b) fluorescence emission spectra of the hemicyanine dyes (5 μM in EtOH). The emission spectrum were obtained by excitation at the maximum absorption wavelength of each dye.

NIR-emitting cyanine dye Indocyanine green (ICG) the dyes here showed larger bathochromic shifts in their absorption and emission maxima

Table 1. Photophysical properties of the hemicyanine (HCy) dyes.

Dye[a]	λ_{abs} (nm)	λ_{em}[b] (nm)	ε ($M^{-1}cm^{-1}$)	Φ_F[c](%) (EtOH)	Φ_F[c](%) (PBS)	Φ_Δ[d] ($^1O_2$) (MeOH)	Stokes shift (nm)
HCy-1	665	725	183,000	0.251	0.185	0.03	60
HCy-2	700	730	323,900	0.312	0.198	0.12	30
HCy-3	710	735	82,300	0.332	0.196	0.09	25
HCy-4	715	740	180,500	0.281	0.184	0.22	25
HCy-5	715	740	84,700	0.345	0.186	0.21	25
HCy-6	720	740	100,200	0.243	0.115	0.80	20
HCy-7	725	785	104,200	0.102	0.084	0.05	60
HCy-8	745	785	232,700	0.113	0.077	0.06	40
ICG[20, 32]	787	818	194,100	0.132	–[e]	~0.009	31

[a]All the measurements were conducted at 25 °C with each of the dyes at 5 μM in EtOH. [b]Measured with excitation at the maximum absorption wavelength in EtOH. [c]The fluorescence quantum yields were determined using Indocyanine green (ICG) in EtOH (Φ_F = 0.132)[20] as a reference. [d]The singlet oxygen quantum yields were determined using Methylene blue in MeOH (Φ_Δ = 0.52)[31] as a reference dye with each of the dyes at 5 μM in MeOH. Singlet oxygen studies were carried out in methanol using 1,3-Diphenylisobenzofuran due to its insolubility in aqueous media. [e] Not determined. Note: ICG absorbs and emits at 787 nm, 818 nm respectively in ethanol.[20]

The effect of pH on the absorption and emission spectra for newly synthesized hemicyanines were examined (Figure S11 and Figure S12) with the absorption maxima for all hydroxyl-substituted hemicyanines (**HCy-OH**) red-shifting with increasing pH due to deprotonation of the phenol leading to enhanced electron donation i.e. the push-pull effect/dipole moment of dyes increased upon increasing pH. Similarly the fluorescence emission intensity also increased with increasing pH (Figure S12). The amino-substituted hemicyanines (**HCy-NH2**) did not show any change in either absorption or fluorescence with changes in pH between 4.0 and 10.0 (Figure S11, S12) due to the pKa value of the aniline.

Applications in potodynamic therapy. Photodynamic therapy (PDT) is popular for the treatment of surface cancers and diseases such as psoriasis. It is based on the use of so-called photosensitizers (PS), with photofrin,[25,26] benzoporphyrin,[27] meta-tetr(hydroxyphenyl)chlorin,[28] N-aspartyl chlorin[29] and Methylene blue,[30] all having been used clinically. The clinically used PS absorb and emit in relatively high wavelength regions

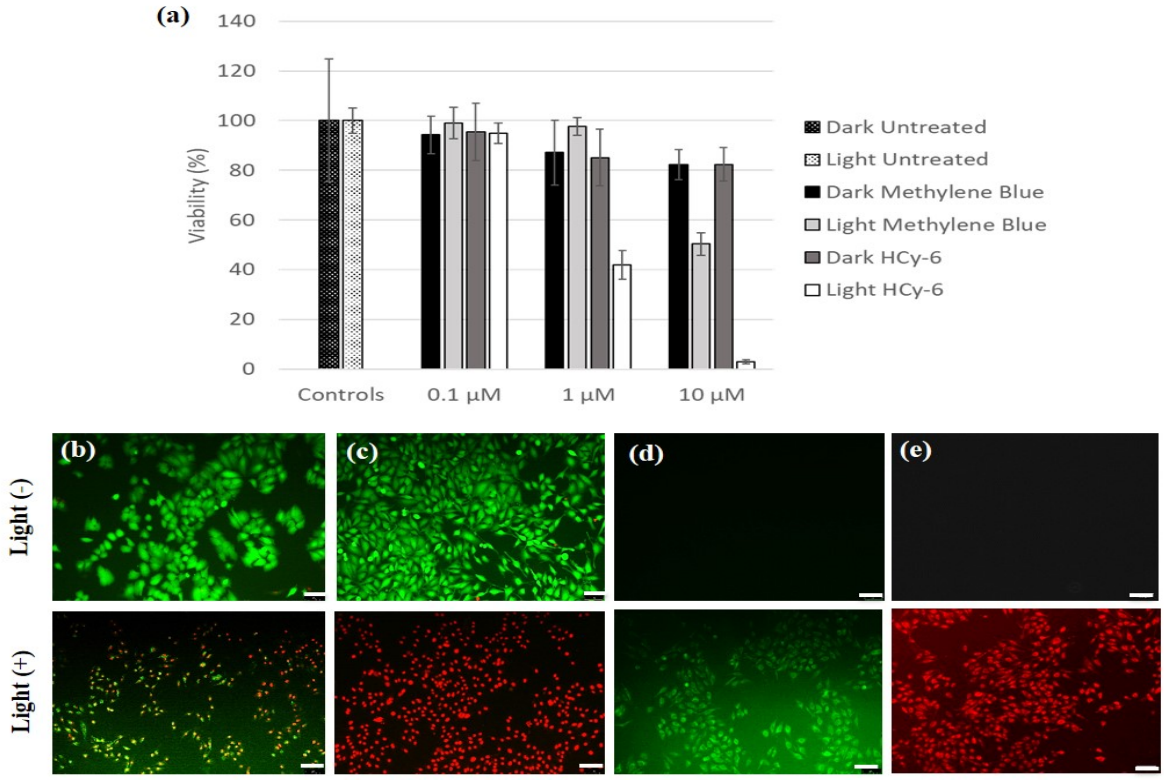

Figure 2. (a) Cell viability of HeLa cells after treatment with three different concentrations of Methylene blue and **HCy-6** with and without irradiation at 640 nm 5 min (n = 3, represents as the mean and standard deviation (SD) of three independent experiments). Live/dead fluorescence microscopy images of HeLa cells after incubation with: (b) Methylene blue (5 uM) and, (c) **HCy-6** (5 uM) with and without irradiation at 640 nm, 5 min (0.01 W/cm^2) using calcein-AM (green) and propidium iodide (red) staining. Fluorescence microscopy images of HeLa cells that have been treated with: (d) the cell permeable dye dichlorofluorescein diacetate (10 μM) and, (e) the dye dihydrorhodamine (10 μM) in the presence of **HCy-6** with and without irradiation at 640 nm for 5 min (0.01 W/cm^2). Scale bar: 100 μm.

(> 630 nm) which is beneficial for biological application, but, the singlet oxygen quantum efficiencies of all of these photosensitizers are moderate (< 0.6). Therefore, there is a real need to develop new PDT agents with longer excitation wavelengths and higher singlet oxygen generation efficiencies. Thus the singlet oxygen quantum efficiencies of all the dyes were analysed (table 1), measuring the changes in absorbance of 1,3-diphenylisobenzofuran at 410 nm in the presence of the hemicyanines (Figure S1 and Figure S2) upon irradiation (0.02 W/cm^2, > 610 nm). The data showed that the dyes with heavy atom substituents had good singlet oxygen quantum efficiencies, with the hemicyanine dye **HCy-6** showing a singlet oxygen quantum efficiency of 0.8, greater than the commercially available dye Methylene blue (Φ_Δ = 0.52),[31] clearly demonstrating for **HCy-6** efficient inter system crossing and subsequent reaction with oxygen. Interestingly **HCy-6** showed higher singlet oxygen quantum efficiency (0.8) than **HCy-4** (0.22) although both are iodo-substituted. Importantly our compounds are significantly better than the NIR-emitting cyanine dye ICG, that has very poor singlet oxygen quantum yield (~0.009), with singlet oxygen quantum efficiency decreasing upon increasing concentration due to aggregation issues.[32] Moreover, there is still a discussion if ICG is actually a photosensitizer or just a chromophore.[33] The generation of other reactive oxygen species (ROS) via a type-II process was also evaluated for **HCy-4**,**5** and **6** using dihydrorhodamine 123 (DHR) (Figure S5, S6, S7 and S8) which transforms into rhodamine 123 with turn-on of fluorescence. Interestingly, **HCy-4**,**5** and **6** all showed turn-on of fluorescence as all generated ROS upon irradiation. Surprisingly, **HCy-5** showed the highest ROS generation efficiency with time compared to **HCy-4** and **HCy-6** (Figure S9) while a control of dihydrorhodamine 123 alone did not show any change of fluorescence upon irradiation in water (Figure S10). Thus **HCy-4**, **HCy-5** and **HCy-6** were all photosensitizers that generated both singlet oxygen ($^1O_2$) and reactive oxygen species (ROS) via type-I and type-II mechanisms. Stability experiments towards oxidants and nucleophiles indicated that **HCy-6** did not show any significant change of its absorption or emission spectra in presence of HOCl, H_2O_2, Cysteine or H_2S (Figure S13).

To evaluate the in vitro singlet oxygen efficiently, the best photosensitizer **HCy-6** was analysed with cells, initially looking at their dark cytotoxicity (CCK-8 assay) with the cells tolerant to **HCy-6** up to 20 μM (Figure S14). As shown in Figure 2a, **HCy-6** significantly inhibited cell proliferation in a dose-dependent manner upon irradiation, with no toxicity was observed in the dark. The "killing efficacy" of **HCy-6** was higher than that of Methylene blue, with a half maximal killing concentration (IC_{50}) of 0.76 μM, some 15 hold lower than that of Methylene blue (Figure S15). The photocytotoxicity of **HCy-6** was further shown by fluorescence microscopy. Thus, HeLa cells were incubated with **HCy-6** or Methylene blue and subjected to illumination. As shown in Figure 2b,c (Figure S16), **HCy-6** lead to almost complete cell death (Figure 2c). Intracellular ROS generation, upon irradiation, was further confirmed with **HCy-6** using the cell permeable reporters (dichlorofluorescein diacetate and dihydrorhodamine 123) with the reduced dyes oxidised by the generated ROS (Figure 2d, e) to give cellular fluorescence. In addition the imaging capability of **HCy-6** was also evaluated with HeLa cells by fluorescence microscopy with results (shown in Figure S17) revealing that **HCy-6** showed high contrast red fluorescence after 2 h of incubation using 1.0 μM dye.

CONCLUSION

In summary new series of hemicyanine dyes were synthesized, which absorb and emit in the NIR region. Dyes with heavy atom substituents **HCy-4**, **HCy-5** and **HCy-6** generated both singlet oxygen ($^1O_2$) and reactive oxygen species (ROS) via type-I and type-II mechanisms. **HCy-6** showed an outstanding singlet oxygen quantum efficiency when illuminated at > 610 nm with a (Φ_Δ = 0.8, with cellular experiments indicating that **HCy-6** showed excellent PDT efficiency that was higher than of commercially available (and clinical used) Methylene blue under identical conditions. Further research on these newly developed photo-sensitizers could allow then to find practical application as photodynamic therapy agents.

ASSOCIATED CONTENT

Supporting Information

The Supporting Information is available free of charge on the ACS Publications website.

Additional figures including singlet oxygen quantum yield measurement, photo-physical property in different organic solvent, dye stability towards oxidant and nucleophiles, photo-physical property in varying pH of medium, ROS generation, cytotoxicity, IC_{50}, all newly synthesized compound's characterization data by 1H and 13C NMR, HPLC, and HRMS data (PDF).

AUTHOR INFORMATION

Corresponding Author

*Mark Bradley – *EaStCHEM School of Chemistry, University of Edinburgh, David Brewster Road, EH9 3FJ, Edinburgh, UK; orcid.org/0000-0001-7893-1575;* Email: mark.bradley@ed.ac.uk

Authors

Mithun Santra – *EaStCHEM School of Chemistry, University of Edinburgh, David Brewster Road, EH9 3FJ, Edinburgh, UK; orcid.org/0000-0003-3165-4659.*

Matthew Owens – *EaStCHEM School of Chemistry, University of Edinburgh, David Brewster Road, EH9 3FJ, Edinburgh, UK; orcid.org/0000-0001-5936-1984.*

Gavin Birch – *EaStCHEM School of Chemistry, University of Edinburgh, David Brewster Road, EH9 3FJ, Edinburgh, UK; orcid.org/0000-0002-8490-6138.*

Author Contributions

The manuscript was written through contributions of all authors.

Notes

The authors declare no competing financial interest.

ACKNOWLEDGMENT

We would like to thank the Medical Research Council grant MR/N02995X/1 and the Engineering and Physical Sciences Research Council (EPSRC), UK for Interdisciplinary Research Collaboration grants EP/K03197X/1 and EP/R005257/1. We thank the BBSRC/GSK for supporting the PhD to Gavin Birch. We thank Dr. Richa Sharma and Paige Shaw for their help in the cells imaging studies.

REFERENCES

(1) Li, X.; Gao, X.; Shi, W.; Ma, H. Design Strategies for Water-Soluble Small Molecular Chromogenic and Fluorogenic Probes. *Chem Rev*. **2014**, *114*, 590−659.
(2) Ueno, T.; Nagano, T. Fluorescent probes for sensing and imaging. *Nat Methods*. **2011**, *8*, 642−645.
(3) Chan, J.; Dodani, S. C.; Chang, C. J. Reaction-based small-molecule fluorescent probes for chemoselective bioimaging. *Nat Chem*. **2012**, *4*, 973−984.
(4) Santra, M.; Jun, Y. W.; Reo, Y. J.; Sarkar, S.; Ahn, K. H. Lavender violet, blue and pink: A new type of benzo[a]phenoxazine-based dipolar, red-emitting dyes. *Dyes and Pigments*. **2017**, *142*, 161−166.
(5) Tansi, F. L.; Ruger, R.; Rabenhold, M.; Steiniger, F.; Fahr, A.; Kaiser, W. A. Liposomal Encapsulation of a Near-Infrared Fluorophore Enhances Fluorescence Quenching and Reliable Whole Body Optical Imaging Upon Activation In Vivo. *Small*. **2013**, *9*, 3659−3669.
(6) Kim, D.; Moon, H.; Baik, S. H.; Singha, S.; Jun, Y. W.; Wang, T. Kim, K. H.; Park, B. S.; Jung, J.; Mook-Jung, I.; Ahn, K. H. Two-Photon Absorbing Dyes with Minimal Autofluorescence in Tissue Imaging: Application to in Vivo Imaging of Amyloid-β Plaques with a Negligible Background Signal. *J. Am. Chem. Soc*. **2015**, *137*, 6781−6789.
(7) Stolik, S.; Delgado, J. A.; Perez, A.; Anasagasti, L. Measurement of the penetration depths of red and near infrared light in human "ex vivo" tissues. *Journal of Photochemistry and Photobiology B*. **2000**, *57*, 90–93.
(8) Weissleder, R.; Ntziachristos, V. Shedding light onto live molecular targets. *Nat. Med*. **2003**, *9*, 123−128.
(9) Koide, Y.; Urano, Y.; Hanaoka, K.; Piao, W.; Kusakabe, M.; Saito, N.; Terai, T.; Okabe, T.; Nagano, T. Development of NIR Fluorescent Dyes Based on Si–rhodamine for in Vivo Imaging. *J. Am. Chem. Soc*. **2012**, *134*, 5029−5031.
(10) Chen, W.; Xu, S.; Day, J. J.; Wang, D.; Xian, M. A General Strategy for Development of Near-Infrared Fluorescent Probes for Bioimaging. *Angew. Chem. Int. Ed*. **2017**, *56*, 16611–16615.
(11) Kolmakov, K.; Hebisch, E.; Wolfram, T.; Nordwig, L. A.; Wurm, C. A.; Ta, H.; Westphal, V.; Belov, V. N.; Hell, S. W. *Chem. Eur. J*. **2015**, *21*, 13344–13356.
(12) Nia, Y.; Wu, J. *Org. Biomol. Chem*. **2014**, *12*, 3774–3791.
(13) Mishra, A.; Behera, R. K.; Behera, P. K.; Mishra, B. K.; Behera, G. B. *Chem. Rev*. **2000**, *100*, 1973−2011.
(14) Ha, T.; Tinnefeld, P. *Annu. Rev. Phys. Chem*. **2012**, *63*, 595–617.
(15) Linde, S. V. D.; Krstic, I.; Prisner, T.; S. Doose, S.; Heilemann, M.; Sauer, M. *Photochem. Photobiol. Sci*. **2011**, *10*, 499–506.
(16) Wang, Y.; Liu, J.; Ma, X.; Cui, C.; Deenik, P. R.; Henderson, P. K. P.; Sigler, A. L.; Cui, L. *Scientific Reports*. **2019**, *9*, 2102.
(17) He, X.; Hu, Y.; Shi, W.; Li, X.; Ma, H. *Chem. Commun*. **2017**, *53*, 9438−9441.
(18) Li, L.; Li, Z.; Shi, W.; Li, X.; Ma, H. *Anal. Chem*. **2014**, *86*, 6115−6120.
(19) He, X.; Li, L.; Fang, Y.; Shi, W.; Li, X.; Ma, H. *Chem. Sci.* **2017**, *8*, 3479−3483.
(20) Rurack, K.; Spieles, M. *Anal. Chem*. **2011**, *83*, 1232–1242.
(21) Adarsh, N.; Avirah, R. R.; Ramaiah, D. *Org. Lett*. **2010**, *12*, 5720−5723.
(22) Mirenda, M.; Strassert, C. A.; Dicelio, L. E.; Roman, E. S. *ACS Appl. Mater. Interfaces*. **2010**, *2*, 1556−1560.
(23) Mujumdar, R. B.; Ernst, L. A.; Mujumdar, S. R.; Lewis, C. J.; Waggoner, A. S. *Bioconjugate Chem*. **1993**, *4*, 105–111.
(24) Ohulchanskyy, T. Y.; Donnelly, D. J.; Detty, M. R.; Prasad, P. N. *J. Phys. Chem. B*. **2004**, *108*, 8668−8672.
(25) Toratani, S.; Tani, R.; Kanda, T.; Koizumi, K.; Yoshioka, Y.; Okamoto, T. *Photodiagnosis and Photodynamic Therapy*. **2016**, *14*, 104–110.
(26) Ormond, A. B.; Freeman, H. S. *Materials*. **2013**, *6*, 817−840.
(27) Joshua, A.; Lai, T. J.; Truitt, A.; Huang, Y. C.; Osannf, K. E.; Choi, B.; Kelly, K. M. *Photodiagnosis and Photodynamic Therapy*. **2009**, *6*, 195−199.
(28) Wennink, J. W. H.; Liu, Y.; Makinen, P.; Setaro, F.; Escosura, A. D. L.; Bourajjaj, M.; Lappalainen, J. P.; Holappa, L. P.; Dikkenberg, J. B. V. D.; Fartousi, M. A.; Trohopoulos, P. N.; Herttuala, S. Y.; Torres, T.; Hennink, W. E.; Nostrum, C. F. V. *European Journal of Pharmaceutical Sciences*. **2017**, *107*, 112–125.
(29) Kato, H.; Furukawa, K.; Sato, M.; Okunaka, T.; Kusunoki, Y.; Kawahara, M.; Fukuoka, M.; Miyazawa, T.; Yana, T.; Matsui, K.; Shiraishi, T.; Horinouchi, H. *Lung Cancer*. **2003**, *42*, 103−111.
(30) Tardivo, J. P.; Giglio, A. D.; Oliveira, C. S; Gabrielli, D. S.; Junqueira, H. C.; Tada, D. B.; Turchiello, D. S. R. F.; Baptista, M. S. *Photodiagnosis and Photodynamic Therapy*. **2005**, *2*, 175−191.
(31) Usui, Y. *Chemistry Letters*. **1973**, 743–744.
(32) Ruhia, M. K.; Ak, A.; Gulsoy, M. *Photodiagnosis and Photodynamic Therapy*. **2018**, *21*, 334–343
(33) Giraudeau, C.; Moussaron, A.; Stallivieri, A.; Mordon, S.; Frochot, C. *Current Medicinal Chemistry*. **2014**, *21*, 1871−1897.